

Equivalent Impedance Analysis and Compensation of Full-wave Bridge Rectifier under High-frequency Operation with Extended Impedance Method

Yichao Liu and Junrui Liang

School of Information Science and Technology, ShanghaiTech University, Shanghai 201210, China

Email: {liuych4, jrliang}@shanghaitech.edu.cn

Abstract—Full-wave bridge rectifiers are widely used in power electronics for ac-dc conversion. In most of the conventional rectifier analysis, the diodes were modeled as unidirectional ideal switches with a constant threshold voltage. Prior knowledge was needed for specifying the on/off state of a diode in different phases, as well as whether the circuit works under continuous or discontinuous condition modes (CCM or DCM). However, under high-frequency operation, whose frequency might be up to several MHz, the influence of parasitic components, such as the junction capacitor, is more significant. Such a simple ideal switch model and preliminary on/off assignment are not accurate enough to describe the actual switching dynamics. Given this insufficiency, this paper proposes an equivalent impedance analysis and compensation study of full-wave bridge rectifiers based on the extended impedance method (EIM). EIM provides an efficient frequency-domain numeric solution for nonlinear circuit analysis. The steady-state characteristics of a rectifier circuit can be easily and efficiently simulated with EIM, no matter it operates in CCM or DCM, under low or high frequencies. Taking the bridge rectifier in the secondary side of a 6.78-MHz wireless power transfer (WPT) system, for example, we demonstrate that EIM can model its dynamics very well. The efficient numeric method is further utilized to optimize the rectifier circuit through impedance compensation towards zero phase angle (ZPA) operation. Both the commercial simulator PSpice and experiment results validate the feasibility of this EIM based analysis and optimization.

I. INTRODUCTION

The full-wave bridge rectifier is an extensively used passive ac-dc power conversion circuit [1]. In many studies, the behaviors of the four diodes in a bridge rectifier are modeled as ideal unidirectional electronic switches, whose specific threshold voltages depend on the semiconducting material, such as silicon, gallium-nitride (GaN), and silicon-carbide (SiC). For an ideal diode, its state is either on or off. Its current and voltage can be formulated with piecewise equations. In the low-frequency operations, such as the piezoelectric [2] and electromagnetic [3] energy harvesting scenarios, the conventional ideal diode model is sufficient to explain the behavior. On the other hand, the bridge rectifier is also used in high-frequency applications, such as the secondary stage of the wireless power transfer (WPT) system. In some up-to-date WPT systems, the switching frequency is up to several MHz, say, 6.78 Mhz [4]. In these cases, even some fast wide bandgap devices, such as SiC diodes, is used, the switching behavior is diverse from idea diodes. The reason comes from the parasitic

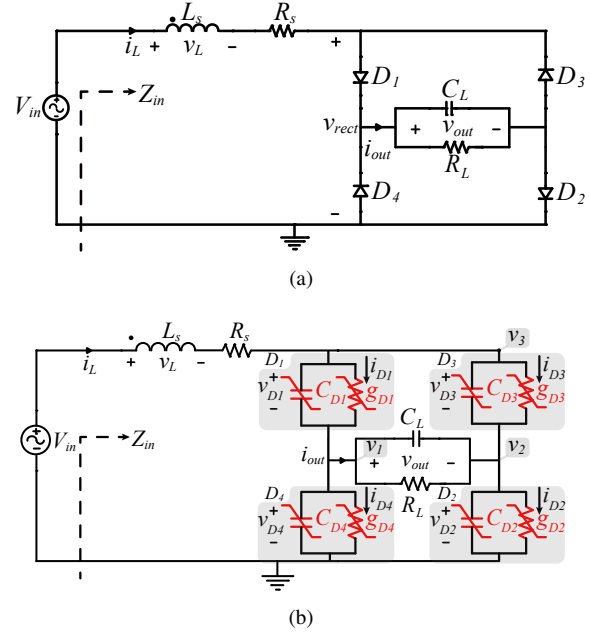


Fig. 1. (a) A full-wave bridge rectifier used in the secondary side of a 6.78 MHz WPT system. (b) Its equivalent EIM model.

components, which exhibit non-negligible influence to the circuit dynamics [5], [6]. The value of nonlinear junction capacitance depends on its voltage in operation; therefore, it is difficult to analytically formulate the steady-state waveform without iterative calculation. The extended impedance method (EIM) [7], [8] expresses all circuit components in complex matrix form. The intuitive EIM offers an efficient tool for formulating and simulating nonlinear circuits. In this paper, we use EIM to study the equivalent impedance of a bridge rectifier and further discuss the impedance compensation towards zero phase angle (ZPA) operation under high-frequency operation.

II. EIM MODEL OF A SINGLE DIODE

As shown in Fig. 1(a), a full-wave bridge rectifier is composed of four diodes, which are intrinsically nonlinear. In this study, each diode is modeled as a parallel combination of its switching conductance and junction capacitance, as shown in Fig. 1(b). In EIM, the dynamic effects of all linear or nonlinear components are modeled as impedance. Taking a

single diode for example, its major I-V characteristics, along the time axis, can be formulated with the Shockley's equation

$$i_d(t) = I_s \left[e^{v_d(t)/(nV_T)} - 1 \right], \quad (1)$$

where I_s is the saturation current, V_T is the thermal voltage, and n is the ideal factor. The equivalent conductance of the diode g_d can be defined as follows

$$g_d[v_d(t)] = \begin{cases} I_s \left[e^{v_d(t)/(nV_T)} - 1 \right] / v_d(t), & v_d < 0, \\ i_d(t) / \{nV_T \ln [i_d(t)/I_s + 1]\}, & v_d \geq 0. \end{cases} \quad (2)$$

Likewise, the junction capacitance in a practical diode, whose dynamic influence becomes more significant under high-frequency operation, can also be formulated as follows

$$c_d[v_d(t)] = \begin{cases} C_{j0} [1 - v_d(t)/V_{bi}]^{-m}, & v_d < 0, \\ C_{j0}, & v_d \geq 0, \end{cases} \quad (3)$$

where C_{j0} is the zero-bias junction capacitance, m is a power efficient, and V_{bi} is the built-in potential. These parameters are all embodied in a SPICE diode model [9].

Since the diode voltage $v_d(t)$ and current $i_d(t)$ are functions of time, from (2) and (3), g_d and c_d can be also regarded as time dependents. This was called *state-to-time mapping* in [8]. On the other hand, the values of g_d and c_d might also changes v_d and i_d in operation. For EIM analysis, iterative calculations are necessary towards the steady-state solution of a circuit involving nonlinear components. The capacitance and conductance in the n^{th} round of calculation are denoted with superscripts, i.e., $c_d^{(n)}(t)$ and $g_d^{(n)}(t)$. The I-V characteristic of the junction capacitance can be formulated in time domain as follows

$$i_d^{(n)}(t) = c_d^{(n)}(t) \frac{dv_d^{(n)}(t)}{dt}. \quad (4)$$

Equation (4) can be converted into a convolution in the frequency domain

$$I_d^{(n)}(j\omega) = c_d^{(n)}(j\omega) * j\omega v_d^{(n)}(j\omega). \quad (5)$$

The admittance matrix of $c_d^{(n)}$, therefore, can be formed in the frequency domain as follows [8]

$$\mathbf{Y}_{c_d}^{(n)} = j\omega_0 \begin{bmatrix} -KC_{d,0}^{(n)} & \cdots & -KC_{d,-K}^{(n)} & \cdots & -KC_{d,-2K}^{(n)} \\ \vdots & \ddots & \vdots & \ddots & \vdots \\ \varepsilon C_{d,K}^{(n)} & \cdots & \varepsilon C_{d,0}^{(n)} & \cdots & \varepsilon C_{d,-K}^{(n)} \\ \vdots & \ddots & \vdots & \ddots & \vdots \\ KC_{d,2K}^{(n)} & \cdots & KC_{d,K}^{(n)} & \cdots & KC_{d,0}^{(n)} \end{bmatrix}, \quad (6)$$

where K is the maximum included harmonics order; $C_{d,k}^{(n)}$ is the Fourier coefficient of the k^{th} harmonic of $c_d^{(n)}(t)$; ε is an infinitesimal number for preventing singularity in matrix manipulation. On the other hand, voltage and current are expressed as vectors in EIM, i.e.,

$$\mathbf{V}^{(n)} = \begin{bmatrix} V_{-K}^{(n)} & \cdots & V_0^{(n)} & \cdots & V_K^{(n)} \end{bmatrix}^T \quad (7)$$

$$\mathbf{I}^{(n)} = \begin{bmatrix} I_{-K}^{(n)} & \cdots & I_0^{(n)} & \cdots & I_K^{(n)} \end{bmatrix}^T \quad (8)$$

TABLE I
SPICE LEVEL 3 MODEL OF DIODE 1N4001

Parameter	Value	Parameter	Value
I_s (Is)	14.11 nA	C_{j0} (Cj0)	25.89 pF
n (N)	1.984	m (M)	0.44
V_T	26 mV	V_{bi} (Vj)	0.3245 V

Therefore, the I-V dynamics of a nonlinear junction capacitance can be derived from (9) to (5).

$$\mathbf{I}^{(n)} = \mathbf{Y}_{c_d}^{(n)} \mathbf{V}^{(n)} \quad (9)$$

Similarly, the admittance matrix of conductance $g_d^{(n)}(t)$ is formulated as follows

$$\mathbf{Y}_{g_d}^{(n)} = \begin{bmatrix} G_{d,0}^{(n)} & \cdots & G_{d,-K}^{(n)} & \cdots & G_{d,-2K}^{(n)} \\ \vdots & \ddots & \vdots & \ddots & \vdots \\ G_{d,K}^{(n)} & \cdots & G_{d,0}^{(n)} & \cdots & G_{d,-K}^{(n)} \\ \vdots & \ddots & \vdots & \ddots & \vdots \\ G_{d,2K}^{(n)} & \cdots & G_{d,K}^{(n)} & \cdots & G_{d,0}^{(n)} \end{bmatrix}. \quad (10)$$

With (6) and (10), the total admittance matrix of a diode can be formulated as follows

$$\mathbf{Y}_d^{(n)} = \mathbf{Y}_{g_d}^{(n)} + \mathbf{Y}_{c_d}^{(n)}. \quad (11)$$

III. EIM MODEL OF A BRIDGE RECTIFIER

Based on (11), the admittance matrices of all four diodes in a bridge rectifier can be formulated in extended impedance expressions. The other linear time-invariant (LTI) components in Fig. 1(b) are modeled as diagonal matrices [2]. The voltages of three nodes in Fig. 1(b), i.e., \mathbf{V}_1 , \mathbf{V}_2 , and \mathbf{V}_3 , in the $(n+1)^{\text{th}}$ iteration therefore can be formulated with KVL and KCL. The governing equation is given by (12), where \mathbf{Y}_{D_x} ($x = 1, 2, 3, 4$) stand for the diode impedance; $\mathbf{Y}_s = \mathbf{Y}_{Ls} \parallel \mathbf{Y}_{Rs}$; $\mathbf{Y}_{load} = \mathbf{Y}_{RL} + \mathbf{Y}_{CL}$. Iteration continues until

$$\left\| \mathbf{V}_{out}^{(n+1)} - \mathbf{V}_{out}^{(n)} \right\|_2 / \left\| \mathbf{V}_{out}^{(n+1)} \right\|_2 < \delta, \quad (13)$$

where $\mathbf{V}_{out}^{(n+1)} = \mathbf{V}_1^{(n+1)} - \mathbf{V}_2^{(n+1)}$; δ is the tolerance, which is selected to be 10^{-10} in this study.

IV. ANALYSIS AND COMPENSATION

Owing to the convenience offered by EIM, a bridge rectifier circuit can be efficiently analyzed and optimized, no matter it operates under either continuous or discontinuous conduction mode (CCM or DCM). Two study cases are provided to validate the analysis.

A. Low-frequency Case

In the first case, a diode bridge, which is composed of normal silicon diodes 1N4001, is used to rectify a 50 Hz ac input. The parameters of 1N4001 are given in Table I. The symbols in parentheses are the corresponding aliases in SPICE.

Define the voltage gain as $G_{vv} = V_{out}/V_{in}$, where V_{out} is the output dc voltage and V_{in} is the input ac magnitude.

$$\begin{bmatrix} \mathbf{V}_1^{(n+1)} \\ \mathbf{V}_2^{(n+1)} \\ \mathbf{V}_3^{(n+1)} \end{bmatrix} = \begin{bmatrix} \mathbf{Y}_{D1}^{(n)} + \mathbf{Y}_{load}^{(n)} + \mathbf{Y}_{D4}^{(n)} & -\mathbf{Y}_{load}^{(n)} & -\mathbf{Y}_{D1}^{(n)} \\ -\mathbf{Y}_{load}^{(n)} & \mathbf{Y}_{D3}^{(n)} + \mathbf{Y}_{load}^{(n)} + \mathbf{Y}_{D2}^{(n)} & -\mathbf{Y}_{D3}^{(n)} \\ -\mathbf{Y}_{D1}^{(n)} & -\mathbf{Y}_{D3}^{(n)} & \mathbf{Y}_{D1}^{(n)} + \mathbf{Y}_s^{(n)} + \mathbf{Y}_{D3}^{(n)} \end{bmatrix}^{-1} \begin{bmatrix} \mathbf{0} \\ \mathbf{0} \\ \mathbf{Y}_s^{(n)} \mathbf{V}_{in}^{(n)} \end{bmatrix} \quad (12)$$

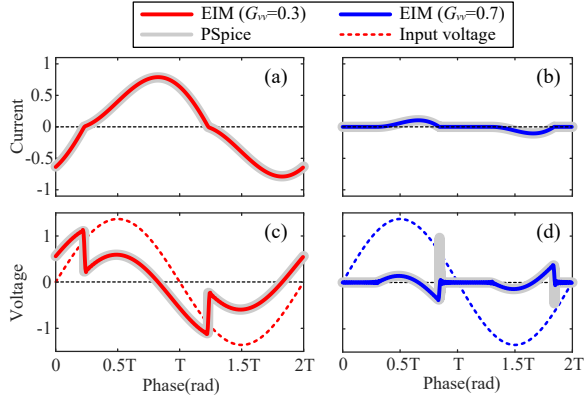


Fig. 2. Inductor normalized voltage and current waveform in low-frequency operation. (a) and (c) CCM operation when $G_{vv} = 0.3$. (b) and (d) DCM operation when $G_{vv} = 0.7$.

The EIM simulation results when $G_{vv} = 0.3$ and $G_{vv} = 0.7$ are shown in Fig. 2. It can be observed that $G_{vv} = 0.3$ corresponds to a CCM case, while $G_{vv} = 0.7$ corresponds to a DCM case. The PSpice results using the same SPICE model listed in Table I validates the modeling accuracy of the EIM based method. However, the PSpice results take about 1.25 and 2.07 seconds to generate in the $G_{vv} = 0.3$ and $G_{vv} = 0.7$ cases, respectively; while EIM takes only 0.21 and 0.24 seconds for the corresponding cases. EIM is more computationally efficient than PSpice simulation.

In conventional studies, the equivalent impedance of a rectifier is usually regarded as purely resistive under low-frequency cases [10]. Therefore, the input impedance Z_{in} in Fig. 1(a) is inductive in general, because of a series inductor L_S . To compensate such an inductive rectifier circuit towards the ZPA target, a series resonant capacitor is usually needed under low-frequency cases.

B. High-frequency Case

In the second case, we study the bridge rectifier behavior under 6.78 MHz operating frequency, in which the junction capacitance plays a non-negligible role. Given the growth of the equivalent capacitive component in the rectifier circuit, the compensation towards ZPA or approaching the unity power factor is more complicated.

1) *Numeric optimization*: Fig. 3 shows the idea of compensation by adding a series compensating impedance Z_{comp} to the circuit. Under harmonic approximation, Z_{comp} should be designed to be the opposite number of the reactance (imaginary part) of Z_{rect} , whose process is shown by the flowchart in Fig. 4(a). Such an optimization might take much iterative effort, since Z_{rect} and Z_{comp} are mutually dependent.

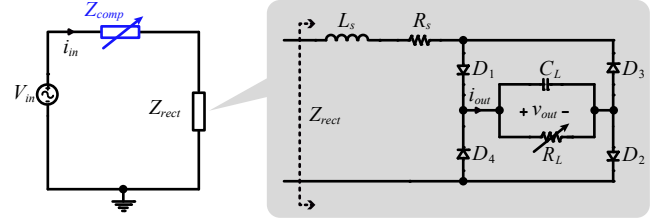


Fig. 3. Tuning Z_{comp} to compensate the impedance of a rectifier circuit.

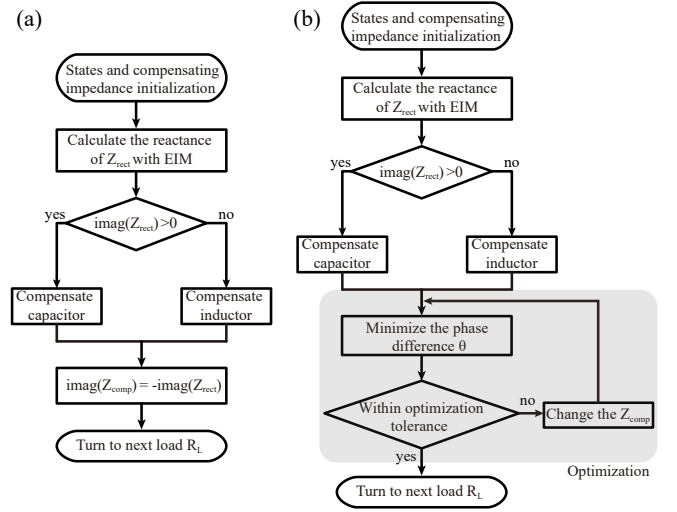


Fig. 4. Flowcharts for calculating compensation impedance Z_{comp} . (a) Reactive (imaginary part) compensation. (b) ZPA optimization.

To simplify the optimization process, this study takes the ZPA criteria, i.e., θ , the phase difference of the voltage and current zero-crossing instants, as the optimization objective. The flowchart of ZPA based optimization is shown in Fig. 4(b).

The different compensating component values under different load R_L values (from 1 Ω to 100 Ω) are numerically solved according to the objective function

$$\min_{Z_{comp}} \theta(Z_{comp}, Z_{rect}, R_L) \quad (14)$$

with a MATLAB built-in function *fminsearch*. The result is briefly shown in Fig. 5. It can be observe that the compensating component should be capacitive in the small R_L region (in blue), while it should be inductive in the large R_L region (in red). It is quite different from the intuitive capacitive compensation in the low-frequency cases.

2) *Experiment*: High-speed SiC diodes are necessary for high-frequency rectification under 6.78 MHz. We use CSD06060 (Cree, Inc.) to build the bridge rectifier in this

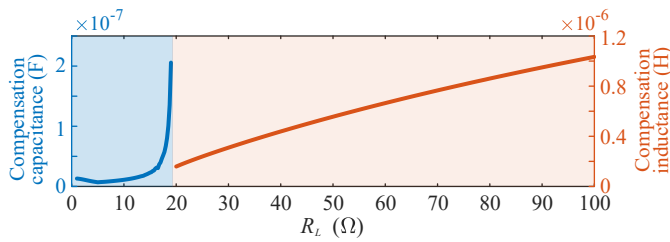


Fig. 5. The value of compensating component towards ZPA operation.

TABLE II
CIRCUIT AND SIMULATION PARAMETERS

	Parameter	Value/Type	Parameter	Value/Type
Circuit	L_s	41.6 nH	R_s	6.25 m Ω
	C_L	10 μ F	V_m	5 V
	D_1 to D_4	CSD06060	n (N)	4.995
	I_s (Is)	479 μ A	C_{j0} (Cj0)	537.33 pF
	V_{bi} (Vj)	0.3905 V	m (M)	0.40753
	Simulation	K	100	N

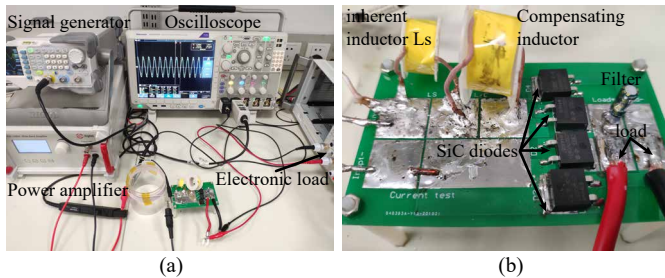


Fig. 6. Experimental setup. (a) Overview. (b) PCB.

case. The circuit and simulation parameters are listed in Table II. V_{in} is the magnitude of the input voltage source. K is the maximum harmonic order. N is the maximum iteration number in EIM.

In order to generate a sinusoidal voltage source with strong loading capacity, a broadband power amplifier and a series LC tank, whose resonant frequency is 6.78 MHz, are used to build the source V_{in} . The experimental setup is shown in Fig. 6(a). The printed circuit board (PCB) prototype is shown in Fig. 6(b), in which a compensating inductor is connected.

Typical operating waveform after compensation when $R_L = 65 \Omega$ and 44Ω are shown in Fig. 7. It can be observed that the input voltage and current are perfectly in phase in both cases.

For all load resistance values from 1Ω to 100Ω , the angle difference and power factor results before and after compensation are comparatively shown in Fig. 8. From Fig. 8(a), we can observe from the black dashed-dot line that θ is positive when $R_L < 20 \Omega$. It means voltage leads current; therefore, the whole circuit is inductive. On the other hand, it is capacitive when $R_L > 20 \Omega$. After the ZPA optimization, the phase difference has been successfully reduced to nearly zero across the load span (solid blue line). The PSpice and experimental results under some specific loading conditions

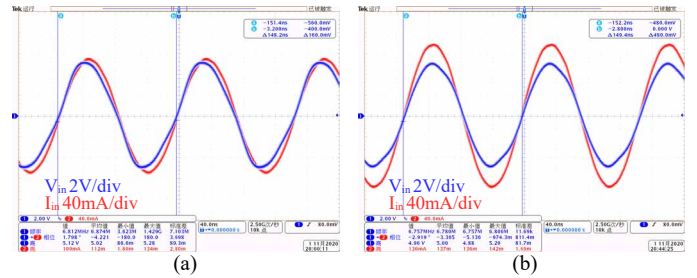


Fig. 7. Input voltage and current waveform after compensation. (a) $R = 65 \Omega$. (b) $R = 44 \Omega$.

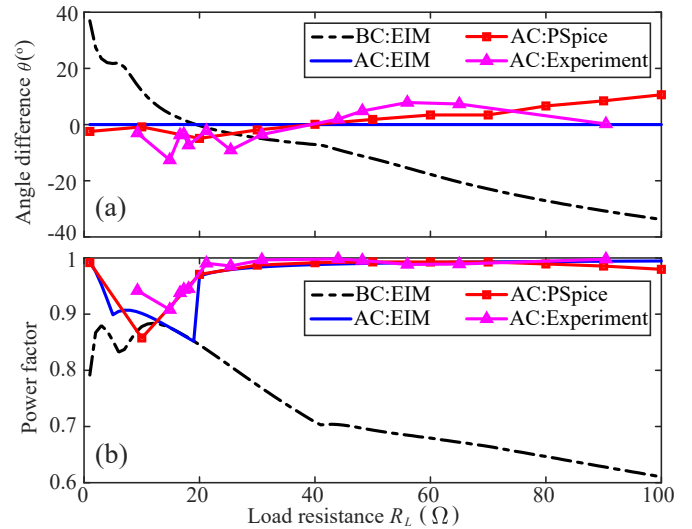


Fig. 8. Compensation results under different load resistance R_L . (a) Phase difference θ between voltage and current. (b) Power factor. (AC: after compensation; BC: before compensation.)

confirm the effectiveness of this optimization. The actual angle difference has been confined within $\pm 10^\circ$. The purpose of ZPA is to increase the power factor. As we can see from Fig. 8(b), after compensation, the power factor has been significantly improved towards unity. In the small R_L region, the power factor is just 0.9. The reason is caused by the high total harmonic distortion (THD) of the input current, although the fundamental harmonic of input voltage and current are almost in phase. This insufficiency can be avoided for higher inherent inductance.

V. CONCLUSION

In this paper, we applied the extended impedance method (EIM), an efficient steady-state numeric simulation method, to analyze the full-wave bridge rectifier working under either low-frequency (50 Hz) or high-frequency (6.78 MHz) conditions. It was found that, when working at high frequency, a rectifier circuit might equivalent to a capacitive or inductive load under different dc loading conditions, which is more complicated than the simple resistive assumption. Efficient EIM numeric analysis helps optimize the power factor towards the zero phase angle (ZPA) criteria within a large load span.

REFERENCES

- [1] R. W. Erickson and D. Maksimovic, *Fundamentals of power electronics*. Springer Science & Business Media, 2007.
- [2] J. Liang and W.-H. Liao, "Impedance modeling and analysis for piezoelectric energy harvesting systems," *IEEE/ASME Transactions on Mechatronics*, vol. 17, no. 6, pp. 1145–1157, 2011.
- [3] J. Liang, C. Ge, and Y.-C. Shu, "Impedance modeling of electromagnetic energy harvesting system using full-wave bridge rectifier," in *Active and Passive Smart Structures and Integrated Systems 2017*, vol. 10164. International Society for Optics and Photonics, 2017, p. 101642N.
- [4] L. Gu, G. Zulauf, A. Stein, P. A. Kyaw, T. Chen, and J. M. R. Davila, "6.78-mhz wireless power transfer with self-resonant coils at 95 % dc–dc efficiency," *IEEE Transactions on Power Electronics*, vol. 36, no. 3, pp. 2456–2460, 2021.
- [5] M. Fu, Z. Tang, and C. Ma, "Analysis and optimized design of compensation capacitors for a megahertz wpt system using full-bridge rectifier," *IEEE Transactions on Industrial Informatics*, vol. 15, no. 1, pp. 95–104, 2018.
- [6] M. H. Rashid, *Power electronics handbook*. Butterworth-Heinemann, 2017.
- [7] J. Liang and W.-H. Liao, "Steady-state simulation and optimization of class-e power amplifiers with extended impedance method," *IEEE Transactions on Circuits and Systems I: Regular Papers*, vol. 58, no. 6, pp. 1433–1445, 2011.
- [8] J. Liang, "Design of class-e power amplifier with nonlinear components by using extended impedance method," in *2016 IEEE International Symposium on Circuits and Systems (ISCAS)*. IEEE, 2016, pp. 437–440.
- [9] M. H. Rashid, *Spice for power electronics and electric power*. CRC press, 2012.
- [10] M. K. Kazimierczuk and D. Czarkowski, *Resonant power converters*. John Wiley & Sons, 2012.